THERMAL MATURITY AND POROSITY DEVELOPMENT DURING CATAGENSIS IN THE BARNETT SHALE, FORT WORTH BASIN, TEXAS

by

NATHAN GLONDYS

Presented to the Faculty of the Graduate School of
The University of Texas at Arlington in Partial Fulfillment
of the Requirements
for the Degree of

MASTER OF SCIENCE IN GEOLOGY

THE UNIVERSITY OF TEXAS AT ARLINGTON
DECEMBER 2011

ACKNOWLEDGEMENTS

I wish to thank the following individuals for their support and guidance: To my mother, Barbara for her love, patience and understanding. To my father, Ronald for instilling a strong work ethic and an innate sense of curiosity and wonder. To my friends, JR and Benita Buzzell. who I owe a debt of gratitude to. To several professors at the University of Texas at Arlington (UTA), Dr. Qinhong Hu (major advisor) who pointed me in the direction needed to start this undertaking, and Drs. John Wickham and Harold Rowe for their invaluable suggestions on the thesis work. And finally, to my mentors and counterparts who have overseen my work, and provided valuable professional and scientific input along the way: Mr. Rick Hoin and Mr. Bill Dees, petroleum geologists with Killam Oil Company in San Antonio and Mr. Rawindra Sutarto, petroleum engineer with Energi Mega Persada in Jakarta, Indonesia.

November 22, 2011

ABSTRACT

THERMAL MATURITY AND POROSITY DEVELOPMENT

DURING CATAGENSIS IN THE BARNETT SHALE,

FORT WORTH BASIN,

TEXAS

Nathan Glondys, M.S.

The University of Texas at Arlington, 2011

Supervising Professor: Qinhong Hu

Unconventional resource plays are typified by significantly recoverable volumes of thermally mature hydrocarbons (oil, condensate and/or gases) trapped within a low permeability shale formation acting as source, reservoir and seal. These systems pose a scientific and engineering challenge to produce recoverable hydrocarbons from, chiefly due to their low permeabilities.

There is growing evidence that secondary porosity in organic gas bearing shales is created during the thermal maturation of kerogen. A better understanding of porosity development during maturation of mobile organics during catagenesis may yield new insight on how we view these systems. A comparative analysis of the gas phase(s), peak gas generation and porosity trends could be used as a screening/diagnostic tool for assessing unconventional

hydrocarbon systems. By comparing regional formation porosity trends against known variations in basin hydrocarbon maturity a relationship might be established.

This study focuses on regional porosity trends in the Barnett Shale of the Fort Worth Basin with respect to constrained variations of known thermal maturity ranges of organic hydrocarbons. Density and neutron porosity well log data from Barnett Shale intervals in selected wells are compared with vitrinite reflectance values and Barnett Shale organic maturation data.

The results of this study indicate that there is a low correlation with measured Barnett Shale formation porosity and areas of increased thermal maturity as determined by vitrinite reflectance.

TABLE OF CONTENTS

LIST OF ILLUSTRATIONS

LIST OF TABLES

CHAPTER 1

INTRODUCTION

1.1 Shale Gas Systems

Unconventional resource plays in the form of shale/mudstone hydrocarbon systems (or self-sourcing low permeability hydrocarbon reservoirs) represent a global energy store which, due to economic and technological limitations, have seen sparse development and exploitation until very recently. Workers have known for several decades that significant volumes of mature hydrocarbons are trapped in these low permeability formations, but these units have been typically bypassed as drilling targets in favor of more readily produced zones (Steward 2007). In the late 1990's, the favorable price of natural gas combined with the implementation of horizontal drilling and hydraulic fracturing, some of these gas shale systems became economically feasible to produce (Bowker 2007).

However, current reservoir stimulation and production methods from these shale systems leave large volumes of unrecovered hydrocarbons left behind. Porosity and pore connectivity are two governing factors in gas deliverability from the reservoir to the wellbore. Production efficiencies vary from play to play and well to well, but are typically less than 15% and usually range between 8%-12% Estimated Ultimate Recovery (EUR) (Curtis 2002).

This study will address the different types of gas phases in the pore network, how maturation of kerogen creates porosity in organic shales and porosity trends in the Barnett Shale across a range of hydrocarbon thermal maturities based on vitrinite reflectance (R_o) data.

1.1.1 Justification

Reservoir parameters such as primary porosity, secondary porosity, effective permeability, reservoir pressures and temperature act in concert and govern the rate and amounts of deliverable hydrocarbons to a wellbore.

Gaseous hydrocarbons are stored in sediments in three phase types: free, adsorbed and dissolved. The free gas phase exists within the void space (pores and fractures); the adsorbed phase as gas molecules adsorbed to the pore walls and as dissolved gas within kerogen and fluids (Curtis 2002).

The work by Jarvie (2004) illustrated a relationship between adsorbed and total gas content with respect to total organic content of the Barnett Shale from the T.P. Sims #2 well, Newark East Field, Fort Worth Basin. Additional work by Wang (2009) highlighted that a significant amount of free gas is stored in the organic matter in productive shale systems. Primary deposition of the rock matrix in shale systems appears to contribute very little to the overall porosity and gas storage. Further work by Loucks (2010) determined that the intraparticle pores in the organic matter are the result of hydrocarbon generation and are a function of the thermal maturity.

The bulk of porosity is these systems appear to be in the organic matter. If the organic matter porosity is created during the maturation of kerogen during catagenesis, then we should see a relationship between regions of higher average porosity and areas correlated with vitrinite reflectance (R_o) data within the peak hydrocarbon generation window.

Further understanding of the relationships of total organic carbon (TOC), gas phases (free, adsorbed, dissolved) and the creation of porosity in organic matter during diagenesis/catagenesis, could lead to better framing of the flow and storage problems of hydrocarbons in shale systems.

1.1.2 Purpose/Objective

The main hypothesis that will be tested is: Are regions of higher thermal maturity associated with higher porosity trends in the Barnett Shale of the Fort Worth Basin?

This hypothesis will be tested by the following approaches:

1) Analyzing the basin evolution of the Fort Worth Basin with respect to the thermal maturation of kerogen and peak gas generation. Thermal maturity information will be based on published R_o values.
2) Utilizing well log and core data to obtain location based porosity information, and
3) Comparing the data sets by overlaying a regional transect of porosity data across a thermal maturity value contour map to see if a correlation exists.

1.1.3 Methods

In natural gas bearing organic shales, porosity is thought to be created during thermal maturation of kerogen (Loucks 2010). The thermal maturity of basins and petroleum systems can be measured with vitrinite reflectance (R_o) data (Magoon 1994; Jarvie 2007). Comparing formation porosity trends across contours of equal R_o intervals may show a relationship between maturity and generated pore space.

The bulk of the analysis in this research will be in processing neutron porosity and density porosity log data and overlaying thermal maturity isoreflectance map based on vitrinite data. Vitrinite data will be obtained from a number of geochemical studies (by Montgomery and others, 2005) and constrained to onset of oil generation (R_o=0.5%) to termination of generation (R_o =1.1%). Porosity data will be gathered from porosity logs (density and neutron) from conventional wireline logs or Measurement While Drilling (MWD) logs from the Texas Railroad Commission. A regional transect consisting of porosity logs that bisects equal R_o contours is then created. This information will then be incorporated as a regional trend map that displays the maturity ranges as well as the porosity trends in the Fort Worth Basin.

CHAPTER 2

REGIONAL SETTING

2.1 Overview of the Fort Worth Basin

Located in North Central Texas, the Fort Worth Basin (Fig. 2.1) is a roughly triangular shaped peripheral foreland basin that is filled with predominantly Paleozoic sediments. Viewed in cross section (Fig. 2.2), this basin is asymmetrical with the deepest portion located adjacent to the western terminus. The tectonic origin and structural evolution of the Fort Worth basin has been discussed in great detail by Walper (1982), Montgomery (2005) and Pollastro (2003). Additionally, the USGS describes the basin as a significant petroleum system encompassing 40 counties of Texas and Oklahoma and having an areal extent of some 54,000 square miles (140,000km^2) (Pollastro 2003).

Figure 2.1 Location and boundaries of the Fort Worth Basin (outlined in red)

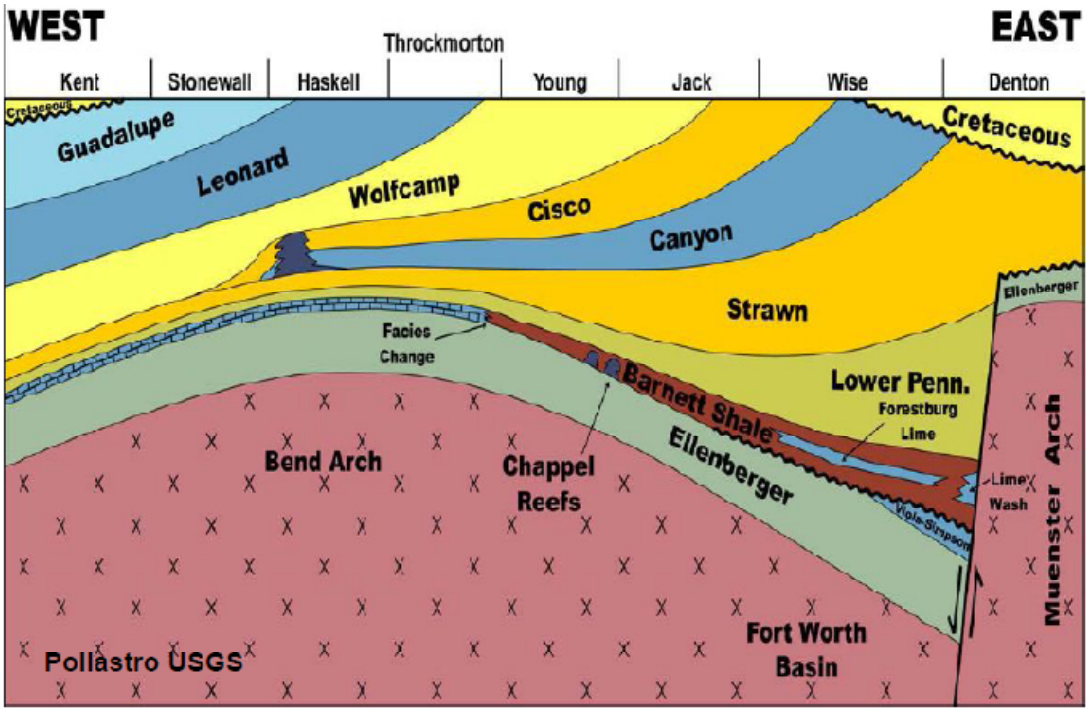

Figure 2.2 The Fort Worth Basin cross section (Pollastro 2003)

2.1.1. Structural Development

The traditionally accepted boundaries of the Fort Worth Basin are large scale regional tectonic features and structural elements (Fig. 2.3). The basin is bounded to the east by the mostly subsurface Ouachita thrust belt which trends northeast-southwest some 200 miles and roughly parallels the Texas Gulf coast. Along the northern edge of the basin, both the Muenster and Red River/Electra Arches are present. The western edge is defined by the Bend Arch and Eastern Shelf of the Permian Basin. The Llano Uplift forms the southern terminus of the basin.

The Fort Worth Basin is one of several basins that formed in response to flexural loading due to the advancing Ouachita thrust belt (Flippen 1982). Initial stages of basin development were preceded by the deposition of shelf edge carbonates along the southern

edge of the North American margin during the Ordovician period. This carbonate platform was then down warped by the thrust loading of the Ouachita orogeny during the Late Paleozoic. The axis of rotation of the eastern portion of the carbonate platform was along several north-south trending hinge lines. These hinge lines migrated westward and are located near the Bend Arch.

Major known regional faults present in the basin include the Mineral Wells and Rhome-Newark fault systems (Steward 2007). These down-to-the-north, normal faults trend NEE-SWW in direction and are approximately 60 miles in length. These faults appear to be associated with the Ordovician Ellenburger and penetrate up to the Cretaceous unconformity.

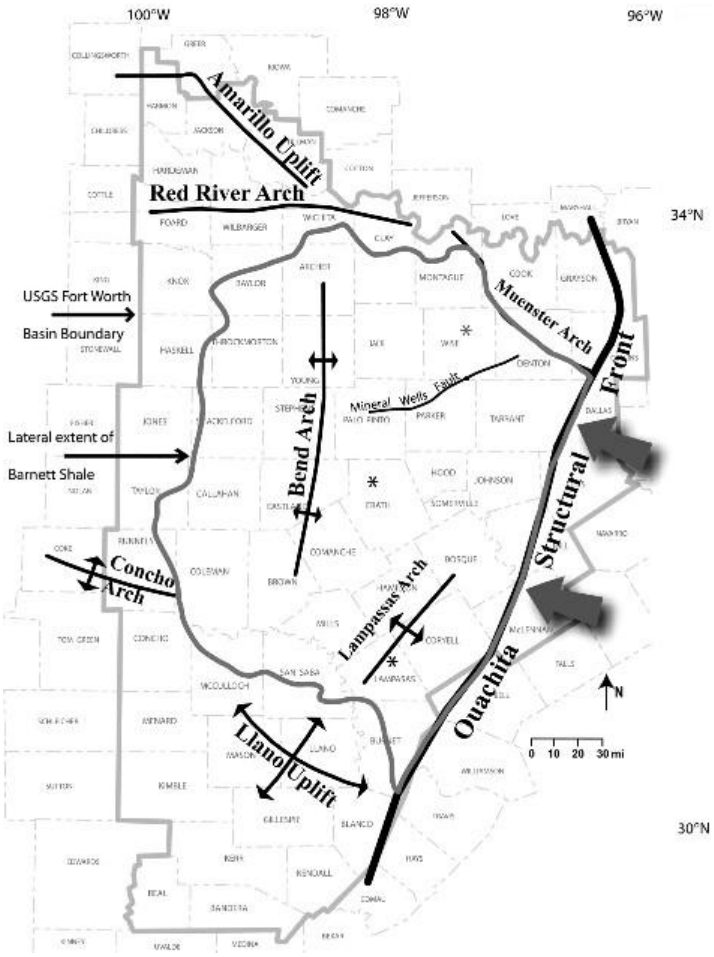

Figure 2.3 Tectonic elements bounding the Fort Worth Basin (Montgomery 2005)

2.1.2. Stratigraphy

A generalized stratigraphic column of the Fort Worth Basin is shown in Figure 2.4. The Paleozoic can be defined by three main intervals based on depositional history as interpreted by Montgomery (2005): 1) Cambrian-Upper Ordovician platform strata, 2) middle and upper Mississippian strata, and 3) Pennsylvanian strata.

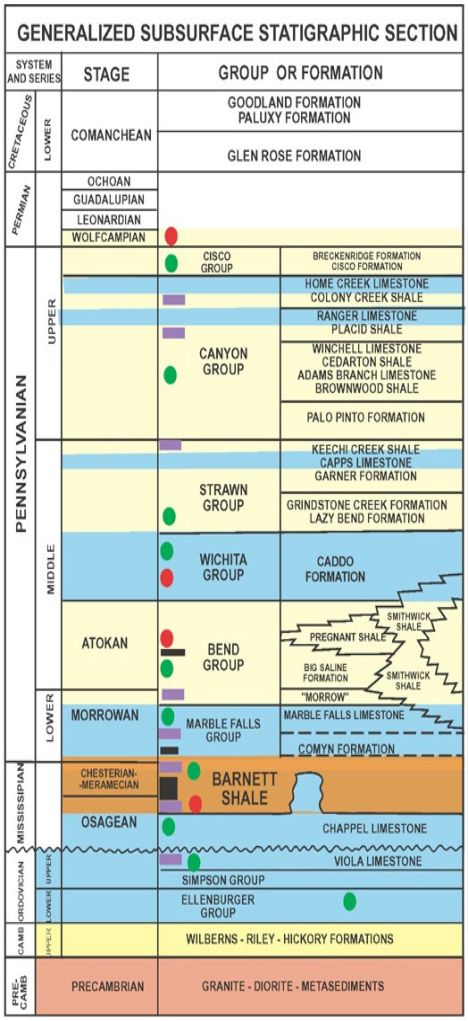

Figure 2.4 Fort Worth Basin Stratigraphy (Pollastro 2003)

The Cambrian-Upper Ordovician platform strata (Ellenburger, Simpson and Viola) are predominately carbonate limestone and dolomites deposited as geographically widespread shelf-edge complexes. The middle and upper Mississippian strata include Chappel Limestone and Barnett Shale that are shallow to deep marine in origin. Pennsylvanian strata (Atoka, Caddo, Strawn, and Canyon) represent extensive terrigenous clastic basin infill deposits that originated from the Ouachita complex.

2.2 Overview of the Barnett Shale

2.2.1. Barnett Shale

The Mississippian Barnett Shale is a dark grey to black, marine shale with a high organic content. The organic matter present in the unit is a type II kerogen capable of generating oil, wet gas and dry gas (Jarvie 2007). This formation was deposited early in basin subsidence (Pollastro 2003) and is classified as two distinct units – the Upper Barnett and Lower Barnett. In the northern part of the Basin the upper and lower units are separated by the Forestburg Limestone. The Forestburg is absent in the southern portion and the upper and lower sections of the Barnett are differentiated by their respective log signatures (see Appendix A – Barnett Shale Type Log).

Table 2.1 Barnett Shale reservoir parameters (Steward 2007)

Gross Lithology	Siliceous mudstone
GIP (BCF/mi^2)	150
Average depth (ft) - subsea	500-7500
Thickness (ft)	100-500
Pressure (psi)	4000
Temperature (F)	200
TOC (%)	4.5
Porosity (%)	6

Table 2.1 - Continued

Permeability (nD)	250
Adsorbed gas (%)	35

Organic shales with higher porosity typically have higher gas productivity due to the fact that produced gas is likely free gas stored in micropores (Zhao 2007).

CHAPTER 3

THERMAL MATURITY, VITRNITE REFLECTANCE AND POROSITY

3.1 Thermal Maturity

Thermal maturation of kerogen is a physicochemical process whereby organic matter is transformed from precursor molecules (proteins, lipids, carbohydrates and nucleic acids) into more complex chains of hydrocarbons. This process involves source rocks containing high amounts of initial organic carbon (>3% wt.) that are subjected to increasing temperatures and pressures. Kerogen transformation is driven by increasing temperature and progresses through several stages that include diagenesis, catagenesis and metagenesis (Fig 3.1). As organic carbon is converted to dead carbon, liquid and gaseous hydrocarbons are produced as reaction products.

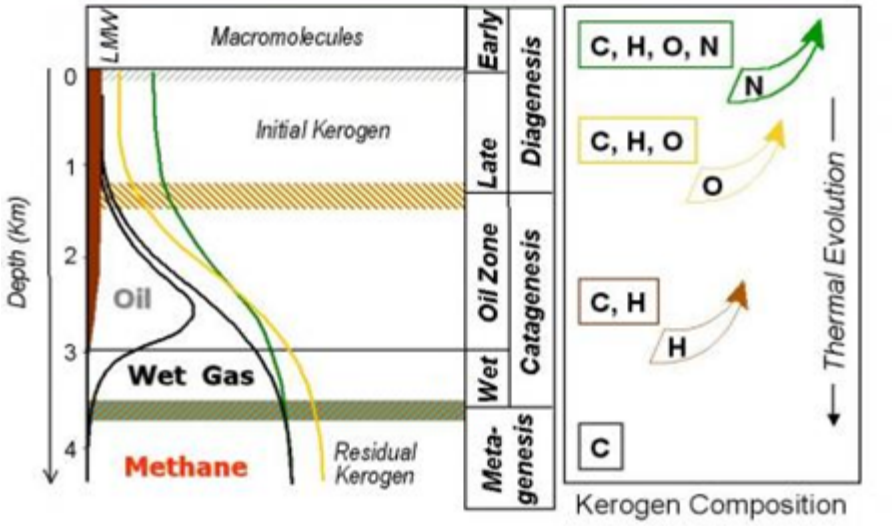

Figure 3.1 Three Stages of Hydrocarbon Generation (modified form Bordenave 1993)

Diagenesis is the initial stage of maturation and begins with the burial and compaction of sediments containing sufficient quantities of organic carbon. Biogenic methane produced from biologic activity is the most common byproduct. Catagenesis is the secondary stage and occurs in the temperature range of 50° to 150°C (12 2° -302°F) and contains the "oil window" and most of the wet "gas window". With increasing temperature, the final stage, metagenesis is reached. This stage occurs at 150° to 200°C (302° -392°F) and produces dry gas (methane and CO_2) and graphite as byproducts.

3.2 Vitrinite Reflectance

The level of maturity (LOM) of petroleum source rocks can be determined by the measurement of vitrinite reflectance (R_o) and can be a useful screening tool that constrains the thermal evolution of a sedimentary basin.

Vitrinite is comprised of organic components (macerals) that make up the physical structure of woody organic materials. Light reflectance measured off of vitrinite increases with higher rank of thermal maturity due to a change in the molecular structure of the macerals (Hunt 1979). The oil window is correlated with a R_o of 0.5% and the gas window begins at a R_o correlation of 0.8%.

Table 3.1 Gas-Prone Generation (modified from Dow 1977)

Generation Stage	R_o (%)
Immature	< 0.8
Early Gas	0.8-1.2
Peak Gas	1.2-2.0
Late Gas	> 2.0

A vitrinite isoreflectance map of the Barnett Shale (see Fig 3.2) highlights a trend of increasing thermal maturity towards the southeast of the basin. (Montgomery 2005)

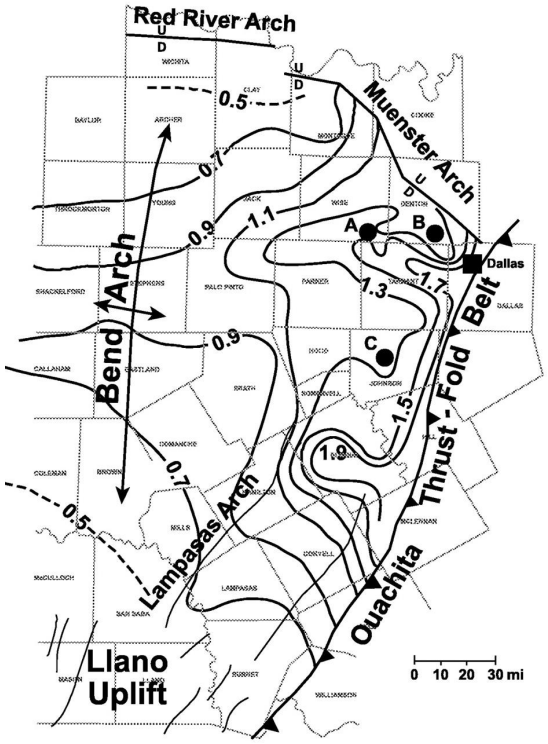

Figure 3.2 Barnett Shale Vitrinite Isoreflectance Map of the Fort Worth Basin (Montgomery 2005)

3.3 Porosity

Formation porosity in wellbores can be determined by either individual porosity log tools (density, neutron, nuclear magnetic resonance or sonic) or by a combination suite of log tools. Utilizing a suite of tools to run through an identical section of formation can correct the for lithology variation effects inherent with readings from individual tools. The most common porosity log suite currently utilized in hydrocarbon exploration is the density porosity (Φ_D) and neutron porosity (Φ_N) log.

Porosity is calculated by the flowing equation:

$$\phi = \frac{\rho ma - \rho b}{\rho ma - \rho f}$$

Where:

$\rho_{b\ is}$ the bulk density

Φ is the porosity

ρ_f is the pore fluid density

ρ_{ma} is the matrix (or particle) density.

Table 3.2 Common Values of Matrix and Fluid Densities (Ellis 2003)

Material	**Density (gm/cc) – ρ_{ma} or ρ_f**
Sandstone	2.65
Limestone	2.71
Dolomite	2.87
Shale	2.58
Kerogen	0.95-1.35
Fresh water	1.00
Salt water	1.2-1.4

True formation porosity may be estimated by taking an average of the density log and neutron log readings by the following equation:

$$\phi = \frac{\sqrt{(\phi N^2 + \phi D^2)}}{2}$$

3.3.1. Porosity from well logs

As stated above, well log derived porosity from the Density tool and the Neutron tool are the most commonly used porosity tools. Neither log measures formation porosity directly. Both tools utilize nuclear methods to ascertain an estimation of formation porosity. Density measurements are made from gamma ray scattering and have a shallow investigation depth. Typical errors arise from the lack of formation contact of the tool sensors due to borehole rugosity. Neutron logs measure the hydrogen content of the formation and are heavily influenced by the presence of water and hydrocarbons.

CHAPTER 4

DATA FROM WELLS

4.1 Methods and Assumptions

The methods utilized for processing and analyzing well log data were as follows: Wells that were drilled in the North Texas, Newark East Field (Barnett Shale) between Jan 1 2000 to Jan 1, 2011, were identified from Texas Railroad Commission files. Gas wells located in the Texas counties of Bosque, Clay, Erath, Hill, Hood, Jack, Montague, Palo Pinto, Parker, Johnson and Somerville (see Fig 4.1 Well Locations) representing roughly a north-south transect through the Fort Worth Basin were utilized. Well logs were chosen and compiled on the basis of tool suite run at the time of logging, with a Gamma log, Neutron Porosity log, and Density Porosity log being preferred. Barnett Shale intervals were then identified (see Appendix A - Barnett Shale Type Log) on the individual well logs. Barnett Shale formation intervals were confirmed with the use of completion data filed at the Texas Railroad Commission by the various operators at the time of gas well completion (see Appendix D – Well Completion Data Example).

Neutron porosity and density porosity values were tallied at 2-foot intervals off of the individual well logs. Average values of neutron porosity and density porosity over the Barnett Shale isolated intervals were then computed. Well coordinates were obtained from the Texas Railroad Commission which has the legal description and latitude and longitude for all permitted oil and gas wells in the state of Texas. Well locations were plotted out and geo-referenced with respect to the Barnett Shale vitrinite isoreflectance map. Porosity values for well locations could then be correlated with known vitrinite values.

4.1.1 Well Data

Complete neutron porosity and density porosity values for each well can be found in Appendix C – WELL DATA.

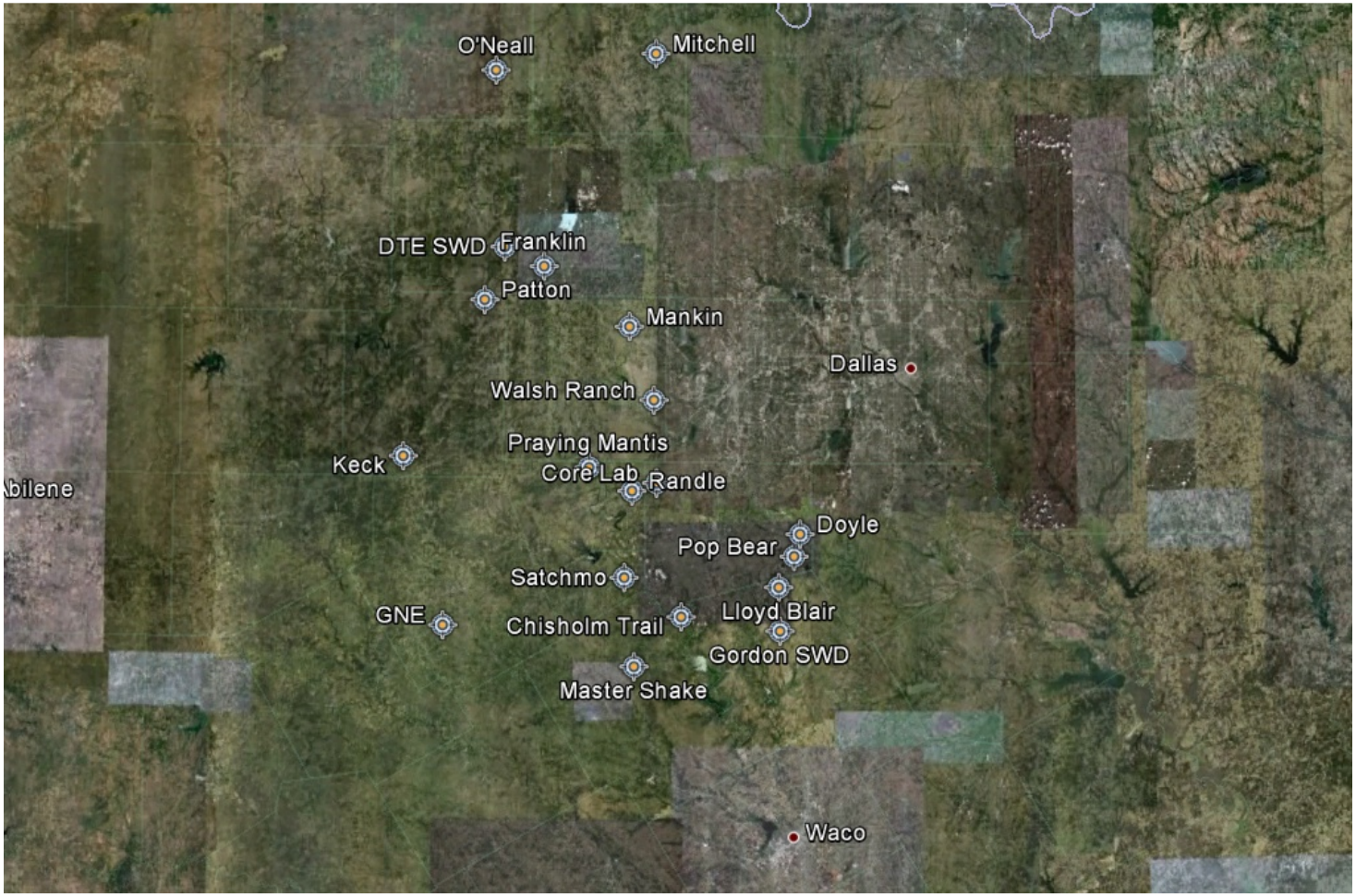

Figure 4.1 Locations of wells for this study

CHAPTER 5

CORRELATION BETWEEN POROSITY AND THEMAL MATURITY

5.1 Results

Comparing the density porosity and neutron porosity values from the above listed wells against the published Barnett Shale Vitrinite Reflectance map from Montgomery yields the following table and figure:

Table 5.1 Summarized Well Log and Vitrinite Data

Well name	**County**	**Ave Φ_N**	**Ave Φ_D**	**Vitrinite Value**
DTE SWD	Jack	18.15	11.93	1.1
Franklin	Jack	15.35	11.8	1.2
Walsh Ranch West	Parker	15.7	5.66	1.2
Mankin	Parker	14.6	8.95	1.4
Core Lab	Johnson	16.51	12.16	1.2
Doyle	Johnson	16.26	7.5	1.9
Pop Bear	Johnson	22.12	9.05	1.9
Lloyd Blair	Hill	16.97	7.13	1.7
Gordon SWD	Hill	17.29	9.47	1.9
Patton	Palo Pinto	20.37	11.27	1.2
Chisholm Trail Ranch	Bosque	16.2	10.2	1.4
Master Shake Unit	Bosque	18.58	9.35	1.5
Randle	Hood	16.41	8.62	1.2
Praying Mantis	Hood	19.51	8.94	1.2
O'Neall	Clay	22.64	13.27	0.7
Satchmo Unit	Somerville	14.79	Not Available	1.35
Keck	Palo Pinto	13.13	10.26	1.0
GNE	Erath	21.89	11.35	0.8
Mitchell	Montague	19.81	10.07	0.9

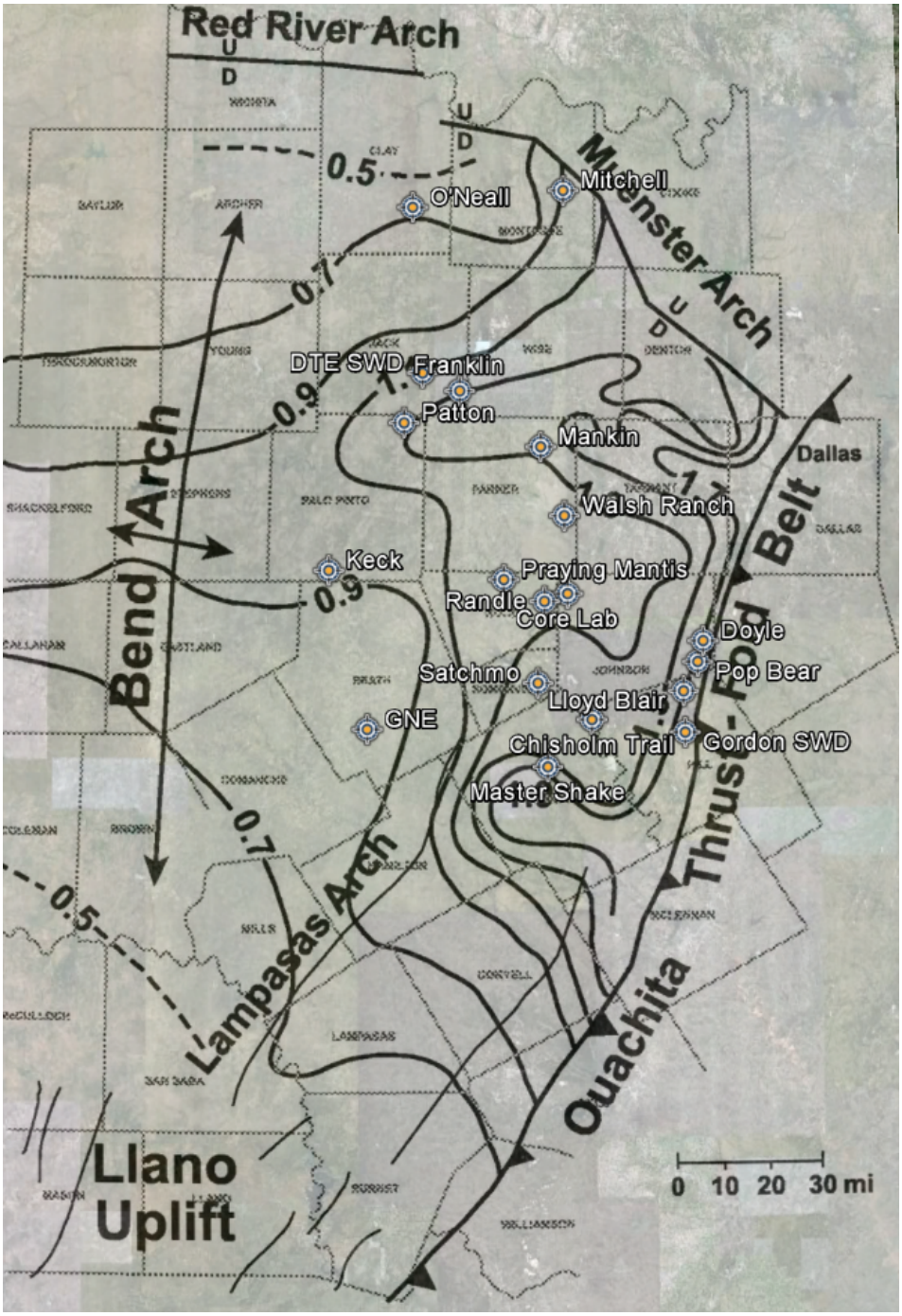

Figure 5.1 Barnett Shale Vitrinite Isoreflectance map and georeferenced well locations (modified from Montgomery 2005)

5.1.1 Relationship between R_o and Porosity

The comparison between averaged density and neutron porosity values of the wells used in this study against known geo-referenced vitrinite values are illustrated in the following graphs (Figs 5.2 and 5.3).

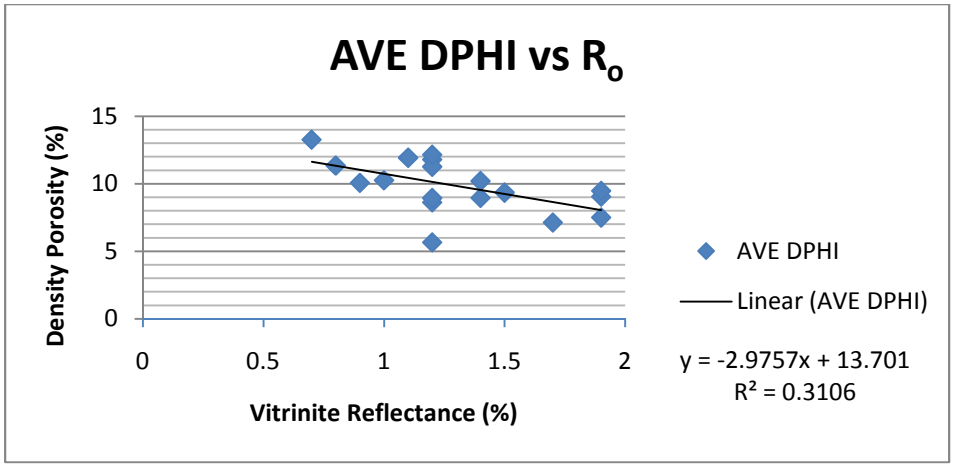

Figure 5.2 Density porosity vs. vitrinite reflectance

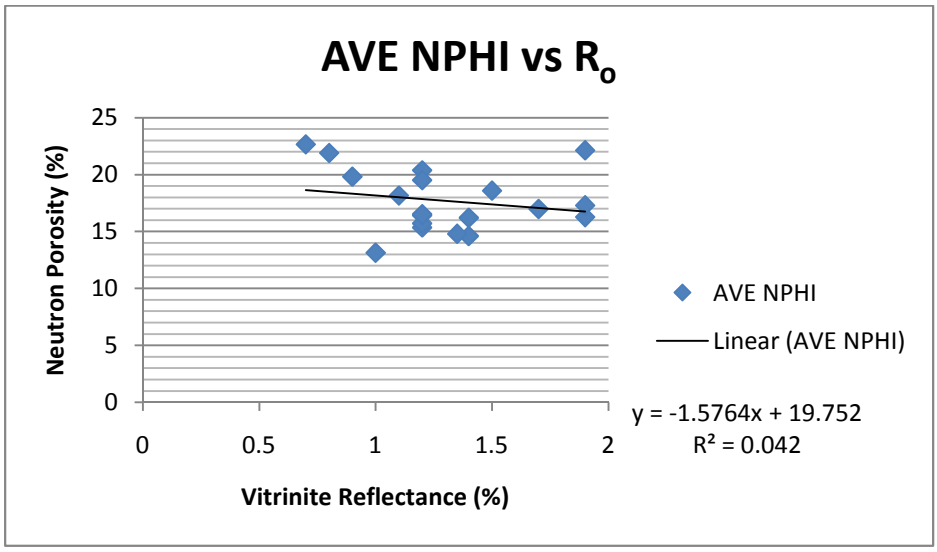

Figure 5.3 Neutron porosity vs. vitrinite reflectance

5.1.2 Relationship between Porosity and Depth

The comparison between averaged density and neutron porosity values of a typical well used in this study against depth values are illustrated in the following graph (Figs 5.4).

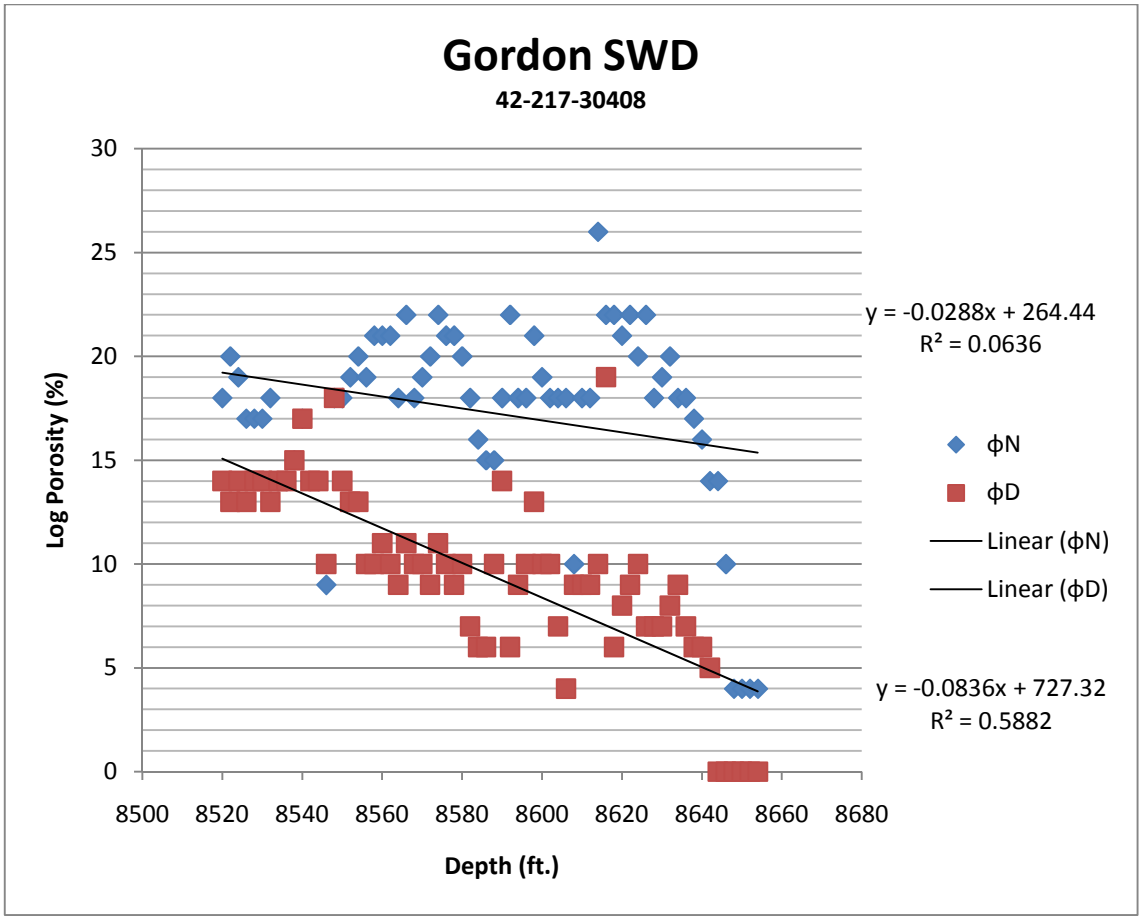

Figure 5.4 Porosity vs. Depth

This decrease in porosity is expected due to the effects of subsidence and overburden weight compacting original porosity.

CHAPTER 6

CONCLUSIONS

Porosity data from the limited number of well logs in this study seems to indicate a slight decrease in measured density porosity and neutron porosity log trends when compared against increasing thermal maturity measured by vitrinite reflectance. This is the opposite of what the author anticipated. This is a potential multivariate problem and several factors are likely to be contributing to the observed results.

The Gordon SWD well porosity vs. depth chart (Figure 5.4) may be highlighting the well documented phenomena of porosity decrease with depth. However, 120 feet of Barnett Shale at approximately 8,500' may not be deep enough or a thick enough section to have such significant effect of loss of porosity (20% loss in N ϕ, and approximately 70% loss in D ϕ) as illustrated by the chart.

Another potential problem could arise with the averaging of porosity over long sections of shale in the individual wellbores. Matrix density differences due to variations in the amounts of TOC maybe masking true densities. Unconverted kerogen and high TOC zones would have much lower density (0.95-1.35 gm/cc) readings when compared to the zones of "pure" shale that would indicate higher densities on the logs (approximately2.58 gm/cc).

Additionally, the number of wells analyzed may not be large enough to establish an accurate and quantifiable trend. Furthermore, the Barnett Shale formation deepens to the eastern portion of the basin and thus has a greater amount of material overlying the unit. Perhaps overburden pressures have greater control over secondary porosity development and/or destruction than the generation of hydrocarbons during thermal maturation of organics. Finally, there may not be any relationship between measured regional formation porosity with well logs and porosity development during catagenesis.

APPENDIX A

BARNETT SHALE TYPE LOG

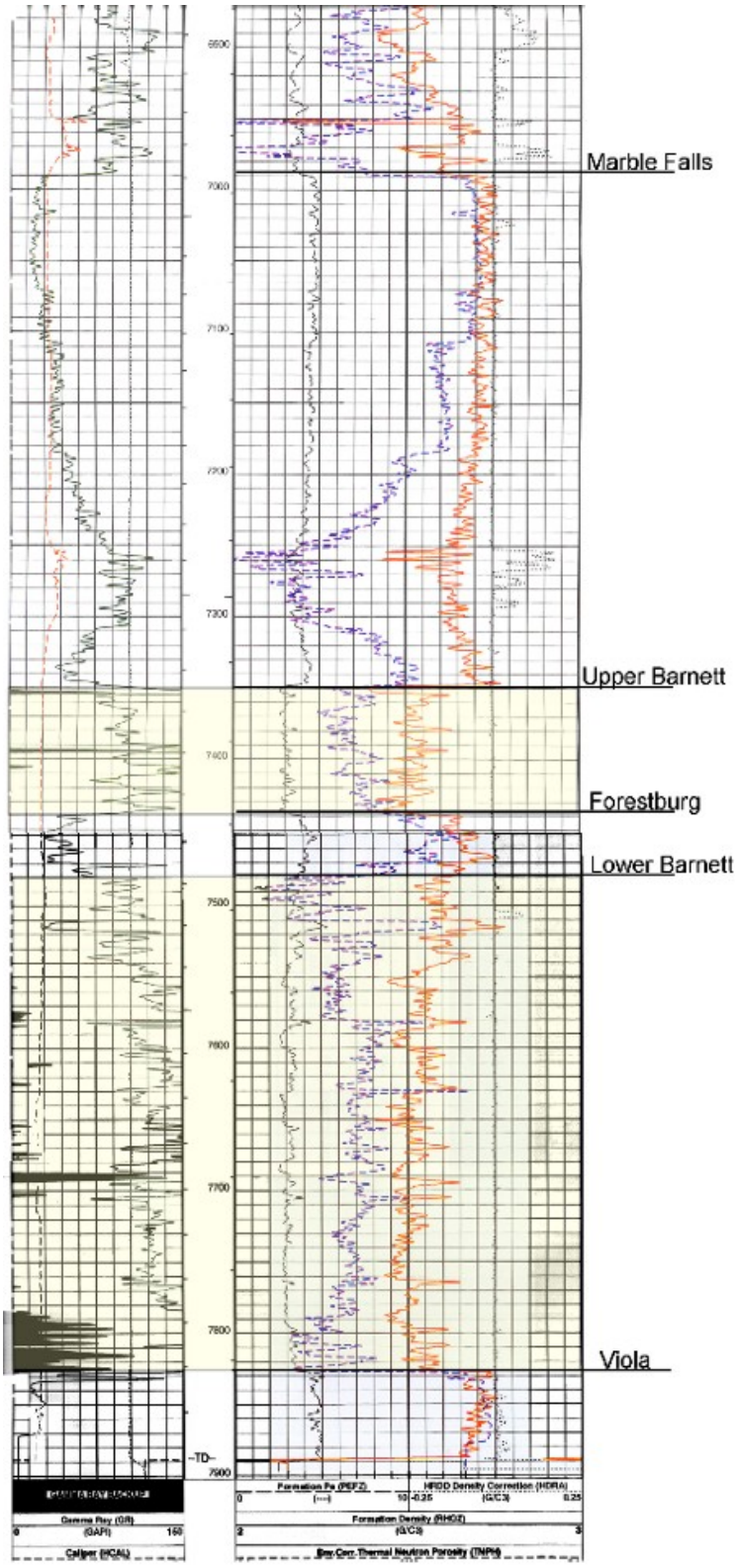
Marble Falls
Upper Barnett
Forestburg
Lower Barnett
Viola
6900
7000
7100
7200
7300
7400
7500
7600
7700
7800
7900
-TD-
Gamma Ray (GR)
(GAPI)
0
150
Caliper (HCAL)
Formation Pe (PEFZ)
0
10
Formation Density (RHOZ)
(G/C3)
2
3
HRDD Density Correction (HDRA)
-0.25
0.25

APPENDIX B

LIST OF ABBREVIATIONS

ABBREVIATIONS

API Number – American Petroleum Institute Well Number; well locatar number in the format 42-251-12345. Where the first two digits are the state (example: 42= Texas), second digits are county (example: 251=Johnson) and the next five are the well number in the county.

BCF – Billion cubic feet

BSMDTOP- Barnett Shale Measured Depth Top

BSMDBOTTOM - Barnett Shale Measured Depth Bottom

E.U.R. – Estimated Ultimate Recovery; total amount of economically recoverable hydrocarbons from a well

GIP – Gas-in-Place

KB – Kelly Bushing

LOM – Level of Maturity

MCF – Thousand Cubic Feet

MMCF – Million Cubic Feet

MD – Measured Depth

MWD – Measurement While Drilling

R_o – Vitrinite Reflectance

SSBSTOP- Sub Surface Barnett Shale Top

TD- Total Depth

TOC – Total Organic Carbon

TVD - Total Vertical Depth

APPENDIX C

WELL DATA

WELLNAME	DTE SWD #1						
API	237-39162						
KB	1211						
BSMDTOP	5920	**SSBSTOP**	-4709				
BSMDBOTTOM	6165						
	Depth(ft)	**Φ_N (%)**	**Φ_D (%)**		**Depth(ft)**	**Φ_N (%)**	**Φ_D (%)**
BSMDTOP	5920	18	10		5986	16	9
	5922	20	12		5988	16	16
	5924	19	12		5990	17	15
	5926	16	11		5992	20	16
	5928	19	14		5994	19	13
	5930	20	16		5996	19	14
	5932	18	16		5998	19	12
	5934	20	12		6000	20	12
	5936	20	14		6002	20	12
	5938	20	14		6004	23	12
	5940	22	14		6006	22	14
	5942	24	14		6008	22	22
	5944	24	7		6010	20	22
	5946	11	5		6012	14	14
	5948	12	8		6014	20	12
	5950	16	16		6016	20	14
	5952	17	15		6018	20	14
	5954	16	10		6020	21	14
	5956	18	13		6022	19	11
	5958	13	13		6024	21	11
	5960	17	8		6026	21	11
	5962	18	8		6028	19	12
	5964	18	9		6030	20	12
	5966	18	14		6032	18	11
	5968	18	15		6034	20	12
	5970	19	16		6036	20	15
	5972	16	14		6038	20	15
	5974	16	15		6040	19	13
	5976	17	10		6042	19	17
	5978	18	10		6044	21	15
	5980	17	14		6046	22	15
	5982	16	8		6048	21	15
	5984	16	9		6050	20	14

WELLNAME	DTE SWD #1	(cont.)					
API	237-39162						
KB	1211						
BSMDTOP	5920	**SSBSTOP**	-4709				
BSMDBOTTOM	6165						
	Depth(ft)	**Φ_N (%)**	**Φ_D (%)**		**Depth(ft)**	**Φ_N (%)**	**Φ_D (%)**
BSMDTOP	6052	22	15		6118	15	14
	6054	21	12		6120	15	12
	6056	16	14		6122	22	9
	6058	13	8		6124	16	7
	6060	18	5		6126	10	5
	6062	20	12		6128	5	10
	6064	20	14		6130	20	10
	6066	20	15		6132	20	10
	6068	22	16		6134	21	10
	6070	23	17		6136	19	10
	6072	23	16		6138	16	8
	6074	21	16		6140	14	6
	6076	20	16		6142	19	8
	6078	21	17		6144	18	8
	6080	18	17		6146	17	6
	6082	19	14		6148	16	4
	6084	19	15		6150	14	5
	6086	21	15		6152	13	4
	6088	20	15		6154	11	0
	6090	20	14		6156	9	0
	6092	18	12		6158	7	0
	6094	20	12		6160	6	0
	6096	20	13		6162	6	0
	6098	21	15		6164	11	0
	6100	23	15				
	6102	20	15				
	6104	19	17				
	6106	19	19				
	6108	21	11				
	6110	20	12				
	6112	22	12				
	6114	21	15				
	6116	17	19				

WELLNAME	Franklin						
API	237-38817						
KB	1054						
BSMDTOP	5790	**SSBSTOP**	-4736				
BSMDBOTTOM	5982						
	Depth(ft)	**Φ_N (%)**	**Φ_D (%)**		**Depth(ft)**	**Φ_N (%)**	**Φ_D (%)**
BSMDTOP	5790	10	10		5856	10	7
	5792	16	15		5858	10	6
	5794	15	14		5860	8	5
	5796	18	17		5862	6	4
	5798	16	18		5864	5	3
	5800	17	17		5866	6	4
	5802	12	13		5868	7	4
	5804	14	12		5870	12	6
	5806	14	14		5872	19	12
	5808	15	14		5874	22	10
	5810	16	13		5876	18	7
	5812	16	12		5878	14	6
	5814	16	14		5880	16	7
	5816	17	14		5882	20	8
	5818	18	13		5884	10	6
	5820	17	12		5886	11	7
	5822	17	14		5888	12	10
	5824	17	15		5890	20	15
	5826	17	13		5892	16	13
	5828	17	12		5894	17	15
	5830	17	12		5896	20	17
	5832	17	14		5898	21	15
	5834	17	16		5900	20	14
	5836	17	14		5902	20	12
	5838	17	12		5904	12	8
	5840	15	12		5906	14	12
	5842	15	13		5908	16	14
	5844	15	14		5910	18	18
	5846	13	13		5912	14	16
	5848	12	11		5914	10	10
	5850	12	12		5916	14	12
	5852	12	11		5918	18	14
	5854	9	7		5920	17	12

WELLNAME	Franklin	(cont.)					
API	237-38817						
KB	1054						
BSMDTOP	5790	**SSBSTOP**	-4736				
BSMDBOTTOM	5982						
	Depth(ft)	**Φ_N (%)**	**Φ_D (%)**		**Depth(ft)**	**Φ_N (%)**	**Φ_D (%)**
BSMDTOP	5922	14	8				
	5924	16	10				
	5926	14	9				
	5928	18	10				
	5930	18	12				
	5932	16	16				
	5934	15	15				
	5936	16	13				
	5938	16	14				
	5940	18	14				
	5942	18	13				
	5944	16	13				
	5946	15	10				
	5948	14	12				
	5950	15	14				
	5952	16	16				
	5954	17	11				
	5956	18	14				
	5958	16	13				
	5960	18	12				
	5962	17	13				
	5964	16	12				
	5966	17	10				
	5968	17	11				
	5970	17	11				
	5972	17	12				
	5974	18	6				
	5976	17	12				
	5978	18	13				
	5980	17	15				
	5982	18	15				

WELLNAME	Walsh Ranch						
API	367-33671						
KB	1018						
BSMDTOP	6598	**SSBSTOP**	-5580				
BSMDBOTTOM	6728						
	Depth(ft)	**Φ_N (%)**	**Φ_D (%)**		**Depth(ft)**	**Φ_N (%)**	**Φ_D (%)**
BSMDTOP	6598	21	10		6664	11	2
	6600	16	9		6666	12	2
	6602	17	12		6668	10	2
	6604	17	9		6670	10	3
	6606	24	10		6672	11	2
	6608	26	15		6674	11	3
	6610	30	15		6676	11	3
	6612	30	12		6678	11	3
	6614	30	13		6680	12	2
	6616	30	17		6682	11	1
	6618	32	14		6684	11	3
	6620	32	12		6686	1	3
	6622	32	10		6688	11	4
	6624	34	11		6690	9	2
	6626	34	14		6692	8	1
	6628	32	11		6694	8	1
	6630	23	12		6696	9	2
	6632	24	8		6698	8	3
	6634	24	12		6700	9	1
	6636	24	12		6702	9	2
	6638	18	9		6704	8	2
	6640	16	7		6706	8	2
	6642	20	12		6708	9	1
	6644	21	11		6710	9	1
	6646	22	10		6712	10	2
	6648	16	4		6714	10	2
	6650	15	5		6716	11	2
	6652	12	3		6718	11	1
	6654	11	0		6720	11	2
	6656	9	0		6722	11	1
	6658	11	3		6724	10	1
	6660	12	3		6726	8	2
	6662	12	3		6728	8	3

WELLNAME	Mankin						
API	367-33883						
KB	951						
BSMDTOP	6559	SSBSTOP	-5608				
BSMDBOTTOM	6736						
	Depth(ft)	Φ_N (%)	Φ_D (%)		Depth(ft)	Φ_N (%)	Φ_D (%)
BSMDTOP	6558	15	14		6624	13	10
	6560	11	4		6626	13	10
	6562	16	8		6628	12	7
	6564	17	12		6630	13	8
	6566	20	10		6632	11	12
	6568	16	6		6634	14	14
	6570	14	6		6636	14	14
	6572	7	2		6638	18	12
	6574	13	8		6640	19	8
	6576	13	12		6642	17	7
	6578	12	12		6644	16	7
	6580	12	12		6646	16	10
	6582	12	8		6648	15	12
	6584	14	7		6650	14	11
	6586	12	9		6652	16	11
	6588	10	6		6654	14	8
	6590	12	8		6656	6	0
	6592	14	8		6658	12	6
	6594	15	7		6660	14	10
	6596	15	8		6662	16	11
	6598	15	10		6664	14	10
	6600	16	10		6666	14	11
	6602	17	11		6668	13	12
	6604	16	11		6670	13	11
	6606	14	10		6672	13	11
	6608	14	13		6674	13	11
	6610	14	8		6676	14	10
	6612	14	7		6678	16	8
	6614	14	11		6680	14	8
	6616	13	11		6682	14	8
	6618	13	10		6684	18	8
	6620	13	7		6686	16	10
	6622	15	10		6688	16	11

WELLNAME	Mankin	(cont.)					
API	367-33883						
KB	951						
BSMDTOP	6559	SSBSTOP	-5608				
BSMDBOTTOM	6736						
	Depth(ft)	Φ_N (%)	Φ_D (%)		Depth(ft)	Φ_N (%)	Φ_D (%)
BSMDTOP	6690	16	10				
	6692	20	9				
	6694	20	9				
	6696	18	10				
	6698	18	13				
	6700	16	6				
	6702	6	4				
	6704	16	4				
	6706	10	6				
	6708	12	2				
	6710	21	6				
	6712	20	6				
	6714	21	8				
	6716	21	10				
	6718	20	4				
	6720	8	4				
	6722	12	9				
	6724	12	8				
	6726	12	6				
	6728	18	8				
	6730	22	18				
	6732	22	19				
	6734	14	14				
	6736	12	0				

WELLNAME	Core Lab						
API	251-30232						
KB	1040						
BSMDTOP	6526	SSBSTOP	-5486				
BSMDBOTTOM	6822						
	Depth(ft)	Φ_N (%)	Φ_D (%)		Depth(ft)	Φ_N (%)	Φ_D (%)
BSMDTOP	6526	11	8		6590	16	13
	6528	16	8		6592	15	13
	6530	11	11		6594	17	12
	6532	13	10		6596	16	13
	6534	16	14		6598	15	12
	6536	15	16		6600	15	12
	6538	15	10		6602	16	12
	6540	18	4		6604	13	10
	6542	17	2		6606	14	10
	6544	12	2		6608	15	11
	6546	12	2		6610	17	13
	6548	16	10		6612	17	12
	6550	15	13		6614	18	12
	6552	15	13		6616	16	13
	6554	17	13		6618	10	7
	6556	18	13		6620	9	6
	6558	18	13		6622	15	14
	6560	19	14		6624	14	14
	6562	16	12		6626	14	12
	6564	11	7		6628	16	14
	6566	16	9		6630	17	15
	6568	17	9		6632	10	8
	6570	22	11		6634	8	8
	6572	19	11		6636	12	11
	6574	18	10		6638	14	12
	6576	16	7		6640	15	14
	6578	20	13		6642	17	14
	6580	14	11		6644	17	16
	6582	12	8		6646	17	15
	6584	14	8		6648	16	11
	6586	18	11		6650	17	11
	6588	16	11		6652	14	15
	6590	16	13		6654	13	15

WELLNAME	Core Lab	(cont.)					
API	251-30232						
KB	1040						
BSMDTOP	6526	SSBSTOP	-5486				
BSMDBOTTOM	6822						
	Depth(ft)	Φ_N (%)	Φ_D (%)		Depth(ft)	Φ_N (%)	Φ_D (%)
BSMDTOP	6656	13	17		6722	16	10
	6658	14	15		6724	19	13
	6660	14	17		6726	20	11
	6662	16	14		6728	13	6
	6664	16	15		6730	18	10
	6666	17	14		6732	21	10
	6668	14	13		6734	21	12
	6670	10	8		6736	22	13
	6672	6	10		6738	21	13
	6674	15	14		6740	19	14
	6676	11	14		6742	17	12
	6678	16	20		6744	16	14
	6680	14	13		6746	15	14
	6682	15	14		6748	15	14
	6684	15	15		6750	16	15
	6686	15	15		6752	16	15
	6688	17	15		6754	18	13
	6690	16	14		6756	16	13
	6692	16	11		6758	15	13
	6694	15	12		6760	17	15
	6696	14	15		6762	17	16
	6698	13	11		6764	17	14
	6700	14	11		6766	16	13
	6702	14	13		6768	18	14
	6704	15	14		6770	19	14
	6706	15	14		6772	21	14
	6708	15	13		6774	16	6
	6710	14	14		6776	18	10
	6712	15	13		6778	20	11
	6714	10	12		6780	21	11
	6716	16	14		6782	20	12
	6718	16	14		6784	20	12
	6720	20	14		6786	21	10

WELLNAME	Core Lab	(cont.)					
API	251-30232						
KB	1040						
BSMDTOP	6526	**SSBSTOP**	-5486				
BSMDBOTTOM	6822						
	Depth(ft)	**Φ_N (%)**	**Φ_D (%)**		**Depth(ft)**	**Φ_N (%)**	**Φ_D (%)**
BSMDTOP	6788	20	11				
	6790	21	12				
	6792	21	12				
	6794	21	13				
	6796	20	13				
	6798	21	14				
	6800	23	13				
	6802	23	14				
	6804	22	14				
	6806	23	13				
	6808	25	15				
	6810	23	14				
	6812	25	14				
	6814	21	13				
	6816	22	13				
	6818	23	13				
	6820	22	16				
	6822	25	12				

WELLNAME	Doyle						
API	251-31190						
KB	699						
BSMDTOP	8358	SSBSTOP	-7659				
BSMDBOTTOM	8460						
	Depth(ft)	Φ_N (%)	Φ_D (%)		Depth(ft)	Φ_N (%)	Φ_D (%)
BSMDTOP	8358	19	11		8424	16	8
	8360	15	10		8426	19	7
	8362	17	7		8428	16	5
	8364	17	0		8430	17	7
	8366	20	8		8432	18	5
	8368	20	8		8434	21	5
	8370	15	10		8436	20	6
	8372	17	10		8438	17	4
	8374	17	10		8440	16	6
	8376	20	10		8442	16	5
	8378	22	12		8444	18	10
	8380	16	5		8446	23	5
	8382	12	5		8448	17	7
	8384	20	11		8450	20	7
	8386	17	8		8452	19	7
	8388	11	10		8454	17	6
	8390	10	10		8456	17	7
	8392	9	11		8458	18	10
	8394	9	10		8460	15	6
	8396	9	10				
	8398	9	7				
	8400	13	6				
	8402	12	10				
	8404	15	5				
	8406	17	7				
	8408	15	6				
	8410	12	5				
	8412	15	8				
	8414	20	10				
	8416	15	3				
	8418	16	9				
	8420	18	8				
	8422	17	7				

WELLNAME	Pop Bear						
API	251-30188						
KB	630						
BSMDTOP	8408	SSBSTOP	-7778				
BSMDBOTTOM	8516						
	Depth(ft)	Φ_N (%)	Φ_D (%)		Depth(ft)	Φ_N (%)	Φ_D (%)
BSMDTOP	8408	21	12		8474	20	11
	8410	21	10		8476	19	10
	8412	22	9		8478	19	7
	8414	26	8		8480	20	10
	8416	24	8		8482	24	12
	8418	21	9		8484	24	10
	8420	22	11		8486	24	6
	8422	23	6		8488	30	12
	8424	27	6		8490	30	13
	8426	25	9		8492	30	8
	8428	24	8		8494	26	9
	8430	25	10		8496	28	12
	8432	23	11		8498	28	9
	8434	23	9		8500	27	9
	8436	25	9		8502	26	8
	8438	23	8		8504	24	7
	8440	22	8		8506	26	7
	8442	21	9		8508	24	8
	8444	20	9		8510	23	8
	8446	18	10		8512	23	7
	8448	17	12		8514	23	6
	8450	15	10		8516	20	0
	8452	13	11				
	8454	13	9				
	8456	14	10				
	8458	16	11				
	8460	20	11				
	8462	17	9				
	8464	13	10				
	8466	17	9				
	8468	21	7				
	8470	23	12				
	8472	24	9				

WELLNAME	Lloyd Blair						
API	217-30381						
KB	727						
BSMDTOP	8098	SSBSTOP	-7371				
BSMDBOTTOM	8518						
	Depth(ft)	Φ_N (%)	Φ_D (%)		Depth(ft)	Φ_N (%)	Φ_D (%)
BSMDTOP	8098	24	4		8164	10	5
	8100	15	0		8166	11	6
	8102	16	3		8168	12	3
	8104	18	3		8170	15	5
	8106	20	6		8172	15	7
	8108	20	4		8174	18	6
	8110	15	0		8176	19	6
	8112	14	2		8178	16	5
	8114	15	3		8180	12	7
	8116	14	3		8182	14	6
	8118	15	4		8184	15	7
	8120	22	9		8186	17	9
	8122	24	6		8188	18	8
	8124	27	6		8190	17	4
	8126	21	2		8192	15	6
	8128	15	3		8194	17	7
	8130	15	3		8196	14	7
	8132	16	4		8198	13	7
	8134	17	6		8200	17	7
	8136	18	4		8202	14	3
	8138	18	3		8204	13	6
	8140	14	5		8206	13	7
	8142	13	5		8208	16	8
	8144	12	6		8210	18	8
	8146	15	5		8212	20	6
	8148	18	5		8214	16	4
	8150	16	2		8216	13	10
	8152	16	2		8218	14	12
	8154	18	4		8220	14	6
	8156	18	5		8222	18	8
	8158	14	6		8224	17	8
	8160	18	6		8226	14	6
	8162	15	3		8228	10	6

WELLNAME	Lloyd Blair	(cont.)					
API	217-30381						
KB	727						
BSMDTOP	8098	SSBSTOP	-7371				
BSMDBOTTOM	8518						
	Depth(ft)	Φ_N (%)	Φ_D (%)		Depth(ft)	Φ_N (%)	Φ_D (%)
BSMDTOP	8230	10	9		8296	16	12
	8232	14	8		8298	15	8
	8234	14	8		8300	19	7
	8236	15	9		8302	20	9
	8238	18	12		8304	19	11
	8240	18	11		8306	19	10
	8242	20	9		8308	20	10
	8244	22	10		8310	16	0
	8246	21	8		8312	15	0
	8248	20	7		8314	18	10
	8250	21	7		8316	18	12
	8252	24	8		8318	15	10
	8254	19	7		8320	15	10
	8256	19	9		8322	19	7
	8258	15	9		8324	15	6
	8260	12	6		8326	10	9
	8262	13	9		8328	10	12
	8264	15	9		8330	9	9
	8266	14	9		8332	10	12
	8268	13	7		8334	10	10
	8270	14	9		8336	11	9
	8272	15	13		8338	11	7
	8274	14	12		8340	13	12
	8276	16	12		8342	15	12
	8278	19	13		8344	19	12
	8280	18	10		8346	16	7
	8282	15	9		8348	21	6
	8284	15	12		8350	21	8
	8286	16	15		8352	21	7
	8288	18	14		8354	21	7
	8290	18	11		8356	21	7
	8292	16	9		8358	20	9
	8294	15	9		8360	19	7

WELLNAME	Lloyd Blair	(cont.)					
API	217-30381						
KB	727						
BSMDTOP	8098	SSBSTOP	-7371				
BSMDBOTTOM	8518						
	Depth(ft)	Φ_N (%)	Φ_D (%)		Depth(ft)	Φ_N (%)	Φ_D (%)
BSMDTOP	8362	19	6		8428	19	8
	8364	18	5		8430	17	13
	8366	15	4		8432	18	9
	8368	18	6		8434	22	5
	8370	16	6		8436	21	9
	8372	16	5		8438	20	9
	8374	18	6		8440	18	8
	8376	19	9		8442	19	6
	8378	19	10		8444	18	9
	8380	19	9		8446	18	9
	8382	17	8		8448	19	10
	8384	17	6		8450	17	9
	8386	18	8		8452	15	9
	8388	18	6		8454	16	8
	8390	21	8		8456	15	9
	8392	22	7		8458	18	10
	8394	22	7		8460	18	9
	8396	19	6		8462	17	9
	8398	21	6		8464	18	9
	8400	19	6		8466	18	9
	8402	17	6		8468	21	10
	8404	18	6		8470	18	9
	8406	20	7		8472	17	6
	8408	19	8		8474	15	5
	8410	18	7		8476	20	8
	8412	17	7		8478	20	8
	8414	18	7		8480	23	6
	8416	18	6		8482	25	9
	8418	16	6		8484	25	10
	8420	6	0		8486	24	10
	8422	6	0		8488	22	9
	8424	15	6		8490	22	9
	8426	19	7		8492	21	8

WELLNAME	Lloyd Blair	(cont.)					
API	217-30381						
KB	727						
BSMDTOP	8098	**SSBSTOP**	-7371				
BSMDBOTTOM	8518						
	Depth(ft)	**Φ_N (%)**	**Φ_D (%)**		**Depth(ft)**	**Φ_N (%)**	**Φ_D (%)**
BSMDTOP	8494	20	9				
	8496	20	5				
	8498	20	7				
	8500	20	7				
	8502	19	5				
	8504	18	6				
	8506	18	7				
	8508	18	7				
	8510	16	4				
	8512	18	3				
	8514	18	5				
	8516	15	0				
	8518	5	0				

WELLNAME	GordonSWD						
API	217-30438						
KB	745						
BSMDTOP	8520	**SSBSTOP**	-7775				
BSMDBOTTOM	8655						
	Depth(ft)	**Φ_N (%)**	**Φ_D (%)**		**Depth(ft)**	**Φ_N (%)**	**Φ_D (%)**
BSMDTOP	8520	18	14		8586	15	6
	8522	20	13		8588	15	10
	8524	19	14		8590	18	14
	8526	17	13		8592	22	6
	8528	17	14		8594	18	9
	8530	17	14		8596	18	10
	8532	18	13		8598	21	13
	8534	14	14		8600	19	10
	8536	14	14		8602	18	10
	8538	15	15		8604	18	7
	8540	17	17		8606	18	4
	8542	14	14		8608	10	9
	8544	14	14		8610	18	9
	8546	9	10		8612	18	9
	8548	18	18		8614	26	10
	8550	18	14		8616	22	19
	8552	19	13		8618	22	6
	8554	20	13		8620	21	8
	8556	19	10		8622	22	9
	8558	21	10		8624	20	10
	8560	21	11		8626	22	7
	8562	21	10		8628	18	7
	8564	18	9		8630	19	7
	8566	22	11		8632	20	8
	8568	18	10		8634	18	9
	8570	19	10		8636	18	7
	8572	20	9		8638	17	6
	8574	22	11		8640	16	6
	8576	21	10		8642	14	5
	8578	21	9		8644	14	0
	8580	20	10		8646	10	0
	8582	18	7		8648	4	0
	8584	16	6		8650	4	0

WELLNAME	GordonSWD	(cont.)					
API	217-30438						
KB	745						
BSMDTOP	8520	**SSBSTOP**	-7775				
BSMDBOTTOM	8655						
	Depth(ft)	**Φ_N (%)**	**Φ_D (%)**		**Depth(ft)**	**Φ_N (%)**	**Φ_D (%)**
BSMDTOP	8652	4	0				
	8654	4	0				

WELLNAME	Patton						
API	363-35625						
KB	1015						
BSMDTOP	5190	SSBSTOP	-4175				
BSMDBOTTOM	5382						
	Depth(ft)	Φ_N (%)	Φ_D (%)		Depth(ft)	Φ_N (%)	Φ_D (%)
BSMDTOP	5190	22	8		5256	20	11
	5192	20	14		5258	18	12
	5194	20	16		5260	21	13
	5196	16	9		5262	22	12
	5198	20	14		5264	20	14
	5200	22	13		5266	22	15
	5202	20	11		5268	23	14
	5204	14	6		5270	22	14
	5206	22	8		5272	25	14
	5208	20	6		5274	23	14
	5210	22	13		5276	23	14
	5212	22	16		5278	25	15
	5214	22	17		5280	24	15
	5216	20	15		5282	24	15
	5218	21	15		5284	24	14
	5220	20	14		5286	23	10
	5222	21	15		5288	26	17
	5224	7	4		5290	26	16
	5226	20	10		5292	24	14
	5228	22	14		5294	24	13
	5230	20	11		5296	21	12
	5232	13	3		5298	24	16
	5234	21	12		5300	22	13
	5236	19	14		5302	23	14
	5238	22	14		5304	24	14
	5240	23	11		5306	24	12
	5242	23	7		5308	24	14
	5244	24	12		5310	23	17
	5246	23	9		5312	19	10
	5248	21	4		5314	23	13
	5250	15	7		5316	23	15
	5252	21	2		5318	24	14
	5254	22	8		5320	23	13

WELLNAME	Patton	(cont.)					
API	363-35625						
KB	1015						
BSMDTOP	5190	SSBSTOP	-4175				
BSMDBOTTOM	5382						
	Depth(ft)	Φ_N (%)	Φ_D (%)		Depth(ft)	Φ_N (%)	Φ_D (%)
BSMDTOP	5322	26	14				
	5324	25	14				
	5326	25	17				
	5328	25	14				
	5330	23	12				
	5332	24	13				
	5334	24	14				
	5336	20	16				
	5338	18	18				
	5340	20	14				
	5342	14	7				
	5344	7	6				
	5346	20	10				
	5348	23	9				
	5350	20	8				
	5352	23	6				
	5354	20	12				
	5356	18	8				
	5358	18	8				
	5360	18	8				
	5362	14	5				
	5364	10	5				
	5366	12	3				
	5368	16	7				
	5370	13	7				
	5372	14	6				
	5374	14	7				
	5376	16	6				
	5378	15	8				
	5380	15	7				
	5382	10	0				

WELLNAME	Chisholm Ranch Trail						
API	035-30138						
KB	648						
BSMDTOP	6580	SSBSTOP	-5932				
BSMDBOTTOM	6669						
	Depth(ft)	Φ_N (%)	Φ_D (%)		Depth(ft)	Φ_N (%)	Φ_D (%)
BSMDTOP	6580	16	16		6644	21	10
	6582	18	16		6646	23	10
	6584	12	14		6648	21	9
	6586	12	16		6650	21	10
	6588	14	14		6652	18	9
	6590	10	10		6654	19	11
	6592	14	13		6656	18	10
	6594	5	5		6658	15	5
	6596	4	4		6660	17	5
	6598	10	10		6662	16	7
	6600	16	15		6664	15	5
	6602	14	11		6666	15	6
	6604	14	12		6668	13	5
	6606	13	11				
	6608	14	8				
	6610	16	14				
	6612	16	13				
	6614	16	13				
	6616	14	13				
	6618	16	11				
	6620	18	14				
	6622	18	10				
	6624	18	9				
	6626	17	9				
	6628	18	9				
	6630	19	10				
	6632	21	8				
	6634	21	10				
	6636	21	10				
	6638	21	10				
	6640	21	10				
	6642	20	10				

WELLNAME	Master Shake						
API	035-30119						
KB	836						
BSMDTOP	5718	**SSBSTOP**	-4882				
BSMDBOTTOM	5812						
	Depth(ft)	**Φ_N (%)**	**Φ_D (%)**		**Depth(ft)**	**Φ_N (%)**	**Φ_D (%)**
BSMDTOP	5718	18	13		5782	23	8
	5720	21	12		5784	21	8
	5722	21	15		5786	24	8
	5724	19	18		5788	24	11
	5726	19	11		5790	22	7
	5728	18	8		5792	23	10
	5730	21	9		5794	21	7
	5732	17	13		5796	24	6
	5734	18	14		5798	24	7
	5736	18	15		5800	20	6
	5738	13	6		5802	19	6
	5740	16	13		5804	17	6
	5742	16	14		5806	16	4
	5744	17	12		5808	15	7
	5746	9	6		5810	15	6
	5748	12	6		5812	3	0
	5750	15	10				
	5752	18	15				
	5754	19	13				
	5756	16	12				
	5758	17	9				
	5760	18	7				
	5762	21	14				
	5764	22	12				
	5766	19	10				
	5768	15	6				
	5770	18	9				
	5772	22	9				
	5774	22	7				
	5776	23	8				
	5778	21	8				
	5780	22	8				

WELLNAME	Randle						
API	221-31219						
KB	965						
BSMDTOP	6272	SSBSTOP	-5307				
BSMDBOTTOM	6500						
	Depth(ft)	Φ_N (%)	Φ_D (%)		Depth(ft)	Φ_N (%)	Φ_D (%)
BSMDTOP	6272	22	13		6338	20	5
	6274	23	11		6340	22	8
	6276	20	12		6342	23	9
	6278	20	16		6344	21	9
	6280	21	14		6346	26	8
	6282	18	13		6348	20	8
	6284	19	15		6350	19	9
	6286	19	15		6352	16	9
	6288	16	11		6354	16	8
	6290	19	16		6356	16	10
	6292	21	16		6358	16	8
	6294	19	17		6360	14	6
	6296	20	19		6362	16	6
	6298	16	16		6364	20	5
	6300	19	10		6366	23	6
	6302	18	13		6368	22	5
	6304	18	14		6370	21	8
	6306	22	13		6372	20	5
	6308	20	13		6374	22	8
	6310	16	6		6376	20	6
	6312	18	12		6378	16	4
	6314	20	10		6380	14	3
	6316	17	11		6382	10	0
	6318	19	11		6384	17	4
	6320	17	7		6386	21	4
	6322	18	12		6388	20	5
	6324	20	10		6390	20	6
	6326	16	11		6392	21	6
	6328	19	13		6394	18	6
	6330	19	8		6396	16	4
	6332	19	5		6398	15	6
	6334	22	7		6400	15	5
	6336	20	7		6402	10	0

WELLNAME	Randle	(cont.)					
API	221-31219						
KB	965						
BSMDTOP	6272	SSBSTOP	-5307				
BSMDBOTTOM	6500						
	Depth(ft)	Φ_N (%)	Φ_D (%)		Depth(ft)	Φ_N (%)	Φ_D (%)
BSMDTOP	6404	5	0		6470	8	2
	6406	5	0		6472	8	2
	6408	5	0		6474	28	22
	6410	8	6		6476	30	23
	6412	14	0		6478	30	23
	6414	8	0		6480	30	23
	6416	7	0		6482	30	24
	6418	8	0		6484	24	10
	6420	7	0		6486	28	16
	6422	3	0		6488	30	23
	6424	0	0		6490	30	22
	6426	4	6		6492	28	25
	6428	6	2		6494	28	22
	6430	2	0		6496	30	22
	6432	4	2		6498	30	25
	6434	2	0		6500	30	20
	6436	0	0				
	6438	4	0				
	6440	6	0				
	6442	4	4				
	6444	7	3				
	6446	6	2				
	6448	5	0				
	6450	5	0				
	6452	3	2				
	6454	5	5				
	6456	7	4				
	6458	7	2				
	6460	12	4				
	6462	26	20				
	6464	26	20				
	6466	8	2				
	6468	11	8				

WELLNAME	Praying Mantis						
API	221-31128						
KB	807						
BSMDTOP	5668	SSBSTOP	-4861				
BSMDBOTTOM	5922						
	Depth(ft)	Φ_N (%)	Φ_D (%)		Depth(ft)	Φ_N (%)	Φ_D (%)
BSMDTOP	5668	26	5		5732	12	7
	5670	22	6		5734	19	10
	5672	18	4		5736	20	9
	5674	14	2		5738	18	12
	5676	10	4		5740	17	10
	5678	14	6		5742	17	12
	5680	20	10		5744	16	14
	5682	22	10		5746	17	14
	5684	22	10		5748	18	12
	5686	21	12		5750	16	8
	5688	21	12		5752	18	12
	5690	21	11		5754	18	12
	5692	21	13		5756	16	10
	5694	21	10		5758	14	6
	5696	21	11		5760	16	9
	5698	20	15		5762	14	12
	5700	19	10		5764	15	12
	5702	19	8		5766	15	10
	5704	18	8		5768	16	6
	5706	16	4		5770	16	10
	5708	18	4		5772	15	9
	5710	21	8		5774	15	9
	5712	14	5		5776	15	8
	5714	18	10		5778	10	9
	5716	18	9		5780	22	9
	5718	18	8		5782	22	9
	5720	18	8		5784	18	8
	5722	18	8		5786	19	8
	5724	11	5		5788	20	8
	5726	12	5		5790	19	9
	5728	18	12		5792	20	10
	5730	18	13		5794	24	10

WELLNAME	Praying Mantis	(cont.)					
API	221-31128						
KB	807						
BSMDTOP	5668	SSBSTOP	-4861				
BSMDBOTTOM	5922						
	Depth(ft)	Φ_N (%)	Φ_D (%)		Depth(ft)	Φ_N (%)	Φ_D (%)
BSMDTOP	5796	21	9		5860	27	10
	5798	20	9		5862	24	8
	5800	19	10		5864	25	10
	5802	19	6		5866	28	9
	5804	20	11		5868	28	10
	5806	19	10		5870	25	10
	5808	19	13		5872	25	10
	5810	16	9		5874	23	7
	5812	18	11		5876	30	9
	5814	20	12		5878	26	9
	5816	21	11		5880	20	9
	5818	18	11		5882	18	9
	5820	20	11		5884	16	9
	5822	14	6		5886	17	12
	5824	22	9		5888	19	8
	5826	18	8		5890	19	9
	5828	20	12		5892	24	12
	5830	18	11		5894	24	12
	5832	19	8		5896	20	10
	5834	20	11		5898	20	9
	5836	23	11		5900	24	9
	5838	20	5		5902	21	9
	5840	21	6		5904	19	10
	5842	21	8		5906	18	8
	5844	21	8		5908	20	6
	5846	21	10		5910	22	8
	5848	21	8		5912	22	8
	5850	22	7		5914	23	6
	5852	25	8		5916	23	6
	5854	23	8		5918	22	5
	5856	28	7		5920	18	5
	5858	28	9		5922	18	2

WELLNAME	ONeall						
API	077-35028						
KB	1029						
BSMDTOP	6356	SSBSTOP	-5327				
BSMDBOTTOM	6456						
	Depth(ft)	Φ_N (%)	Φ_D (%)		Depth(ft)	Φ_N (%)	Φ_D (%)
BSMDTOP	6356	23	21		6422	23	17
	6358	24	13		6424	24	15
	6360	23	16		6426	23	11
	6362	24	15		6428	24	10
	6364	25	17		6430	25	10
	6366	26	20		6432	24	11
	6368	25	17		6434	21	14
	6370	26	18		6436	17	14
	6372	30	17		6438	18	15
	6374	30	17		6440	24	15
	6376	27	16		6442	21	9
	6378	25	13		6444	13	5
	6380	24	11		6446	15	6
	6382	24	12		6448	18	9
	6384	23	12		6450	21	7
	6386	24	14		6452	21	3
	6388	24	13		6454	6	2
	6390	24	15		6456	2	3
	6392	25	16				
	6394	21	27				
	6396	24	18				
	6398	23	17				
	6400	24	16				
	6402	21	9				
	6404	24	13				
	6406	26	12				
	6408	24	11				
	6410	24	12				
	6412	24	12				
	6414	26	15				
	6416	27	16				
	6418	26	15				
	6420	25	15				

WELLNAME	Satchmo						
API	425-30117						
KB	765						
BSMDTOP	5780	SSBSTOP	-5015				
BSMDBOTTOM	5895						
	Depth(ft)	Φ_N (%)	Φ_D (%)		Depth(ft)	Φ_N (%)	Φ_D (%)
BSMDTOP	5780	12	NR		5844	17	NR
	5782	16	NR		5846	15	NR
	5784	21	NR		5848	13	NR
	5786	19	NR		5850	10	NR
	5788	21	NR		5852	10	NR
	5790	20	NR		5854	10	NR
	5792	22	NR		5856	8	NR
	5794	21	NR		5858	10	NR
	5796	22	NR		5860	12	NR
	5798	21	NR		5862	14	NR
	5800	22	NR		5864	15	NR
	5802	24	NR		5866	12	NR
	5804	24	NR		5868	10	NR
	5806	27	NR		5870	9	NR
	5808	25	NR		5872	7	NR
	5810	24	NR		5874	6	NR
	5812	22	NR		5876	5	NR
	5814	21	NR		5878	4	NR
	5816	20	NR		5880	3	NR
	5818	21	NR		5882	9	NR
	5820	20	NR		5884	15	NR
	5822	15	NR		5886	10	NR
	5824	8	NR		5888	4	NR
	5826	16	NR		5890	4	NR
	5828	20	NR		5892	3	NR
	5830	18	NR		5894	1	NR
	5832	16	NR				
	5834	19	NR				
	5836	17	NR				
	5838	16	NR				
	5840	17	NR				
	5842	15	NR				

*NR-tool not run

WELLNAME	Keck						
API	363-35415						
KB	928						
BSMDTOP	3750	**SSBSTOP**	-2822				
BSMDBOTTOM	3840						
	Depth(ft)	**Φ_N (%)**	**Φ_D (%)**		**Depth(ft)**	**Φ_N (%)**	**Φ_D (%)**
BSMDTOP	3750	13	4		3816	14	14
	3752	6	7		3818	15	11
	3754	7	12		3820	15	13
	3756	11	7		3822	13	15
	3758	16	8		3824	13	16
	3760	13	5		3826	13	16
	3762	12	5		3828	13	13
	3764	15	2		3830	14	9
	3766	15	7		3832	15	10
	3768	15	8		3834	14	12
	3770	13	6		3836	13	11
	3772	15	12		3838	13	9
	3774	15	12		3840	13	9
	3776	13	7				
	3778	13	15				
	3780	14	14				
	3782	18	13				
	3784	10	10				
	3786	10	9				
	3788	13	12				
	3790	17	14				
	3792	12	12				
	3794	7	7				
	3796	14	10				
	3798	11	7				
	3800	14	9				
	3802	15	9				
	3804	15	11				
	3806	16	14				
	3808	15	15				
	3810	12	12				
	3812	7	7				
	3814	14	12				

WELLNAME	GNE						
API	143-31151						
KB	1301						
BSMDTOP	3796	SSBSTOP	-2495				
BSMDBOTTOM	3940						
	Depth(ft)	Φ_N (%)	Φ_D (%)		Depth(ft)	Φ_N (%)	Φ_D (%)
BSMDTOP	3796	15	6		3862	10	6
	3798	25	7		3864	5	9
	3800	24	15		3866	15	9
	3802	25	20		3868	24	12
	3804	21	8		3870	21	14
	3806	19	11		3872	22	13
	3808	25	6		3874	24	12
	3810	1	0		3876	24	12
	3812	25	10		3878	25	9
	3814	27	15		3880	26	10
	3816	25	15		3882	27	11
	3818	15	5		3884	29	12
	3820	15	10		3886	30	12
	3822	20	15		3888	30	16
	3824	21	16		3890	30	18
	3826	16	16		3892	29	17
	3828	17	17		3894	30	15
	3830	21	17		3896	30	15
	3832	23	10		3898	30	15
	3834	10	6		3900	30	14
	3836	15	11		3902	28	13
	3838	19	11		3904	26	11
	3840	21	15		3906	22	8
	3842	24	11		3908	21	10
	3844	23	9		3910	30	14
	3846	24	13		3912	26	13
	3848	23	15		3914	25	12
	3850	24	14		3916	27	12
	3852	18	12		3918	23	13
	3854	20	9		3920	23	12
	3856	22	15		3922	19	9
	3858	19	12		3924	22	7
	3860	21	12		3926	23	9

WELLNAME	GNE	(cont).					
API	143-31151						
KB	1301						
BSMDTOP	3796	**SSBSTOP**	-2495				
BSMDBOTTOM	3940						
	Depth(ft)	**Φ_N (%)**	**Φ_D (%)**		**Depth(ft)**	**Φ_N (%)**	**Φ_D (%)**
BSMDTOP	3928	22	12				
	3930	21	12				
	3932	22	8				
	3934	22	7				
	3936	21	9				
	3938	15	3				
	3940	6	0				

WELLNAME	Mitchell						
API	337-33708						
KB	1116						
BSMDTOP	7462	**SSBSTOP**	-6346				
BSMDBOTTOM	7590						
	Depth(ft)	**Φ_N (%)**	**Φ_D (%)**		**Depth(ft)**	**Φ_N (%)**	**Φ_D (%)**
BSMDTOP	7462	13	2		7528	18	14
	7464	14	2		7530	24	15
	7466	18	2		7532	24	14
	7468	22	6		7534	26	14
	7470	22	8		7536	26	11
	7472	23	9		7538	24	13
	7474	22	9		7540	22	7
	7476	22	6		7542	20	7
	7478	18	6		7544	22	10
	7480	14	6		7546	18	2
	7482	26	11		7548	11	1
	7484	18	10		7550	16	2
	7486	18	2		7552	20	6
	7488	23	10		7554	25	9
	7490	22	13		7556	26	10
	7492	20	12		7558	23	11
	7494	20	13		7560	23	11
	7496	24	15		7562	23	12
	7498	22	18		7564	26	14
	7500	23	18		7566	22	15
	7502	22	12		7568	15	14
	7504	20	11		7570	17	5
	7506	19	13		7572	21	11
	7508	21	12		7574	17	6
	7510	19	13		7576	16	11
	7512	21	15		7578	11	8
	7514	18	18		7580	14	11
	7516	11	6		7582	19	11
	7518	22	14		7584	17	11
	7520	21	14		7586	20	14
	7522	21	14		7588	23	12
	7524	18	10		7590	11	6
	7526	11	7				

APPENDIX D

WELL COMPLETION DATA EXAMPLE

Type or print only
483-04

330/0, 320/20 ac.

RAILROAD COMMISION OF TEXAS
Oil and Gas Division

Form G-1
Rev. 4/1/83
EAG0897

API No. 42-367-~~33612~~ 33712

Gas Well Back Pressure Test, Completion or Recompletion Report, and Log

1. FIELD NAME (as per RRC Records or Wildcat) Newark, East (Barnett Shale)	2. LEASE NAME Walsh Ranch West	7. RRC District No. 9
3. OPERATOR'S NAME (exactly as shown on Form P-5, Organization Report) XTO Energy Inc.	RRC Operator No. 945936	8. RRC Gas ID No. 241543
4. ADDRESS 210 West 6th Street. Ste 1005, Fort Worth, TX 76102		9. Well No. 6 3H
5. Location (Section, Block, and Survey) ac.5 HT & B RR Co., A647	5b. Distance and direction to nearest town in this county. 2 miles North East of Aledo	10. County of well site Parker
6. If operator has changed within last 60 days, name former operator	12. If workover or reclass, give former field (with reservoir) & Gas ID or oil lease no. FIELD & RESERVOIR / GAS ID or OIL LEASE # / Oil -- O Gas -- G / WELL #	11. Purpose of filing Initial Potential ☐ Retest ☐ Reclass ☐ Well record only (Explain in remarks) ☒
13. Pipe Line Connection Barnett Gathering		
14. Completion or recompletion date Waiting on Pipeline	15. Any condensate on hand at time of workover or recompletion? ☐ Yes ☒ No	16. Type of Electric or other Log Run. Gamma

Section I — GAS MEASUREMENT DATA

Date of Test

Gas measurement Method (Check One) Orifice Meter ☐ ▶ Flange Taps ☐ Pipe Taps ☐ Positive Choke ☐ Orifice Vent Meter ☐ Pitot Tube ☐ Critical-flow Prover ☐

Gas produced during test MCF

Run No.	Line Size	Orif. or Choke Size	24 Hr. Coeff. Orif. or Choke	Static P_m or Choke Press	Diff h_w	Flow Temp. °F	Temp. Factor F_{tf}	Gravity Factor F_g	Compress Factor F_{pv}	Volume MCF/DAY
1										
2										
3										
4										

Section II — FIELD DATA AND PRESSURE CALCULATIONS

Gravity (Dry Gas)	Gravity Liquid Hydrocarbon Deg. API	Gas-Liquid Hydro Ratio CF/Bbl	Gravity of Mixture G_{mix} =	Avg. Shut-in Temp. °F	Bottom Hole Temp. °F @

$D_{eff}^{8/3}$ = $\sqrt{T_f}$ = $\sqrt{\quad}$ = $\sqrt{GL}$ = $\sqrt{\quad}$ =

$C = \frac{1118 \times (D_{eff})^{8/3}}{\sqrt{T}}$ = = $\frac{\sqrt{GL}}{C}$ = =

RECEIVED
CENTRAL RECORDS
JAN 24 2007
AUSTIN, TEXAS

Run No.	Time of Run Min.	Choke Size	Wellhead Press. PSIA P_w	Wellhead Flow Temp. °F	P_w^2 (Thousands)	R	R^2 (Thousands)	P_l	P_w / P_l
Shut-In									
1									
2									
3									
4									

Run No.	F	K	$S = \frac{1}{z}$	Eks	P_f and P_s	P_f^2 and P_s^2 (Thousands)	$P_f^2 - P_s^2$ (Thousands)	Angle of Slope θ n Absolute Open Flow MCF/DAY
Shut-In								
1								
2								
3								
4								

RECEIVED
R.R.C. OF TEXAS
MAY 19 2006
OIL & GAS DIVISION
WICHITA FALLS, TEXAS

WELL TESTER'S CERTIFICATION: I declare under penalties prescribed in Sec. 91.143, Texas Natural Resources Code, that I conducted or supervised the test and that data and facts shown in Sections I and II above are true, correct, and complete, to the best of my knowledge. Bottomhole temperature and the diameter and length of flow string were furnished by the operator of the well.

Signature: Well Tester — Name of Company: XTO Energy, Inc. — RRC Representative

OPERATOR'S CERTIFICATION: I declare under penalties prescribed in Sec. 91.143, Texas Natural Resources Code, that I am authorized to make this report, that I prepared or supervised and directed this report, and that data and facts stated therein are true, correct, and complete, to the best of my knowledge.

Signature: Operator's representative — Kelly Canada-Young — Title: Reg. Compl. Asst. — Date: 5/11/2006 — Tel: 817-885-3136 A C Number

62

VALID PERMIT

JUL 31 2006

SECTION III — DATA ON WELL COMPLETION AND LOG (Not Required on Retest)

17. Type of Completion:	New Well [X]	Deepening [ ]	Plug Back [ ]	Other [ ]	
18. Permit to Drill, Plug Back or Deepen	DATE 12/20/2005	PERMIT NO. 559017			
19. Notice of Intention to Drill this well was filed in Name of: XTO Energy Inc.	Rule 37 Exception	CASE NO.			
	Water Injection Permit	PERMIT NO.			
	Salt Water Disposal Permit	PERMIT NO.			
	Other	PERMIT NO.			

R.C.C. LETTER DATED 12-16-05

Depth 875 + 20 ft.

Surface Casing 980 ft.

O.W.U.

20. Number of producing wells on this lease in this field (reservoir) including this well	21. Total number of acres in this lease	22. Date Plug Back, Deepening, WorkOver or Drilling Operations: Commenced	Completed	23. Distance to nearest well, Same Lease & Reservoir
11	6307.22	1/3/2006	1/25/2006	2204

24. Location of well, relative to nearest lease boundaries of lease on which this well is located	Feet From	Line and	Feet from
	602 North	West Line of the Walsh Ranch West	1095 Lease

25. Elevation (DF, RKB, RT, GR, ETC.)	26. Was directional survey made other than inclination (Form W--12)?	
1006	[X] Yes	[ ] No

27. Top of Pay	28. Total Depth	29. P.B. Depth	30. Surface Casing Determined by:				Dt. of Letter
	8611MD 6642TVD		Field Rules [ ]	Recommendation of T.D.W.R. Railroad Commission (Special) [X]			12-16-05 Dt. of Letter

31. Is well multiple completion?	32. If multiple completion, list all reservoir names (completions in this well) and Oil Lease or Gas ID No. FIELD & RESERVOIR	GAS ID or OIL LEASE#	Oil--O Gas--G	WELL #	33. Intervals Drilled by:	Rotary Tools	Cable Tools
[ ] Yes [X] No						X	

34. Name of Drilling Contractor	35. Is Cementing Affidavit Attached?
Patterson UTI Drilling	[X] Yes [ ] No

36. CASING RECORD (Report All Strings Set in Well)

CASING SIZE	WT#/FT.	DEPTH SET	MULTISTAGE TOOL DEPTH	TYPE & AMOUNT CEMENT (sacks)	HOLE SIZE	TOP OF CEMENT	SLURRY VOL. cu. ft.
9 5/8"	36#	980	--	365 sxs Class C	12 1/4	surface	630
5 1/2"	17#	8611.3	--	640 sxs class H	8 3/4	5951	890

37. LINER RECORD

Size	TOP	Bottom	Sacks Cement	Screen

38. TUBING RECORD

Size	Depth Set	Packer Set
	6675'	

39. Producing Interval (this completion) Indicate depth of perforation or open hole

From	To
7205'	8518'

40. ACID, SHOT, FRACTURE, CEMENT SQEEZE, ETC.

Depth Interval	Amount and Kind of Material Used
8247' - 8518'	15336 bbls sw w/264200# 30/70 + 73000# 20/40 wsd
7726' - 7997'	15312 bbls sw w/264200# 30/70 + 73000# 20/40 wsd
7205' - 7476'	15287 bbls sw w/264200# 30/70 + 73000# 20/40 wsd

41. FORMATION RECORD (LIST DEPTHS OF PRINCIPAL GEOLOGICAL MARKERS AND FORMATION TOPS)

Formations	Depth	Formations	Depth
Bend Conglomerate	5798'		
Marble Falls	6453'		
Barnett	6598'		

REMARKS Waiting on pipeline
Requesting Lease ID Number

X = 1,972,318
Y = 384,222 NAD 27

REFERENCES

Bordenave, M.L., 1993. Applied Petroleum Geochemistry. Editions Technip, Paris

Bowker, K.A. 2007. Barnett Shale gas production, Fort Worth Basin: Issues and discussion. AAPG Bulletin, v. 91, pp. 523-533.

Bustin, R.M., et al. 2008. Impact of Shale Properties on Pore Structure and Storage Characteristics. SPE-119892, paper presented at Shale Gas Production Conference, SPE, Fort Worth, TX, November 16-18.

Curtis, J., 2002. Fractured shale-gas systems. AAPG Bulletin, v.86, pp.1921-1938.

Dow, W. 1977. Kerogen studies and geological interpretations. Journal of Geochemical Exploration, Volume 7, Issue C, Pages 79-99

Ellis, D., 2003, Formation Porosity Estimation from Density Logs. Petrophysics, v.44, no.5, p.306-316.

Flippen, J.W., 1982, The Stratigraphic, structure, and economic aspects of the Paleozoic strata in Erath County, north-central Texas, in C.A. Martin, ed., Petroleum Geology of the Fort Worth Basin and Bend Arch area: Dallas Geological Society, pp. 129-177.

Hill, R. J., D. Jarvie, J. Zumberge, M. Henry, and R. Pollastro 2007. Oil and gas geochemistry and petroleum systems of the Fort Worth Basin. AAPG Bulletin, v. 91, pp.445-473.

Hill, R.J., E. Zhang, B.J. Katz, and Y.C. Tang. 2007. Modeling of gas generation from the Barnett Shale, Fort Worth Basin, Texas. AAPG Bulletin, v. 91, pp. 501-521.

Hunt, J., 1979. Petroleum Geochemistry and Geology. W.H. Freeman and Company, San Francisco, CA.

Jarvie, D., 2004. Evaluation of Hydrocarbon Generation and Storage in the Barnett Shale, Fort Worth Basin, Texas: The University of Texas at Austin, Bureau of Economic Geology/PTTC, 116p.

Jarvie, D., R. Hill, T. Ruble and R. Pollastro, 2007, Unconventional shale-gas systems: The Mississippian Barnett Shale of north-central Texas as one model for thermogenic shale-gas assessment: AAPG Bulletin, v.91, p.475-499.

Loucks, R. G. , S.C.Ruppel. 2007. Mississippian Barnett Shale: Lithofacies and depositional setting of a deep-water shale-gas succession in the Fort Worth Basin, Texas. AAPG Bull., v. 91; (4), pp. 579-602.

Loucks, R.G., et al. 2010. Preliminary Classification of Matrix Pores in Mudrocks. Gulf Coast Association of Geological Societies Transactions, v. 60, pp. 435-441.

Loucks, R.G., et al. 2009. Morphology, Genesis and Distribution of Nanometer-Scale Pores in Siliceous Mudstones of the Mississippian Barnett Shale. Journal of Sedimentary Research 79: 848-861.

Magoon, L. and W. Dow. 1994. The Petroleum System from Source to Trap. AAPG Memoir 60,Tulsa, OK.

Montgomery, S., D. Jarvie, K. Bowker, and R. Pollastro, 2005, Mississippian Barnett Shale, Fort Worth basin, north-central Texas: Gas-shale play with multi-trillion cubic foot potential: AAPG Bulletin, v.89, p.155-175.

Pollastro, R., R. Hill, T. Ahlbrandt, R. Charpentier, T. Cook, T. Klett, M. Henry, and C. Schenk, 2003, Assessment of Undiscovered oil and gas resources of the Bend-Arch-Fort Worth Basin province of North Central Texas and Southwestern Oklahoma, U.S. Geological Survey Fact Sheet 2004-3022, 2p.

Steward, D., 2007, The Barnett Shale Play: Phoenix of the Fort Worth Basin. A History. F. Paniszczyn, ed., The Fort Worth Geological Society. pp.202.

Walper, J., 1982, Plate Tectonic Evolution of the Fort Worth Basin, in C.A. Martin, ed., Petroleum Geology of the Fort Worth Basin and Bend Arch area: Dallas Geological Society, p. 237-251.

Wang, F.P. and Reed, R.M., 2009. Pore Networks and Fluid Flow in Gas Shales. SPE-124253, paper presented at the Annual Technical Conference and Exhibition, SPE, New Orleans, LA, October 4-7.

Zhao, H., N. Givens and B. Curtis, 2007, Thermal Maturity of the Barnett Shale determined from well-log analysis: AAPG Bulletin, v.91, p.535-549.

BIOGRAPHICAL INFORMATION

Nathan Glondys is a petroleum geologist who, at the time of this writing, is employed by Killam Oil Company, Ltd. in San Antonio, Texas. Mr. Glondys has been a geologist for over a decade and has worked on numerous geological, geophysical and subsurface investigations and projects. Mr. Glondys is currently interested in the recovery of natural gas and liquid hydrocarbons from conventional and unconventional resources. His current focus is the production of natural gas from tight gas sands and shales in South Texas Gulf Coast region.

Mr. Glondys received his Bachelor of Science in Geology from Arizona State University in Tempe, Arizona and is a member of the American Association of Petroleum Geologists, South Texas Geological Society, and Houston Geological Society.